Solvent Effect on Reaction Mechanism and Kinetics of Triplet Ion Pairs between Chloranil and Acenaphthene

Harumichi KOBASHI,* Shunichi OKABE, Youichi OHSUGI, and Haruo SHIZUKA
Department of Chemistry, Faculty of Engineering, Gunma University, Kiryu, Gunma 376
(Received March 22, 1990)

A comparative study on decay dynamics of triplet ion pairs has been performed for the chloranil (CA) and acenaphthene (ACN) system in both the nonpolar solvent benzene (BZ) and the moderately polar 1,2-dichloroethane (DCE) by means of nanosecond laser photolysis. Triplet chloranil (^{3}CA) is quenched by ACN to yield the (1 : 1) triplet ion pair (IP_1), $^3(CA^{\cdot-}, ACN^{\cdot+})$, in BZ, while the (1 : 2) ion pair (IP_2), $^3(CA^{\cdot-}, ACN_2^{\cdot+})$, in DCE as well as IP_1 in the concentration range less than 1 M (1 M=1 mol dm^{-3}) of ACN. Temperature dependence of the transient spectra indicates that IP_2 is energetically lower than IP_1 in DCE. In BZ, IP_1 decays through both back electron transfer (back ET) to the ground state of the donor-acceptor pair and intra-ion-pair proton transfer (PT) leading to formation of the chloranil semiquinone radical (CAH·). In DCE, both IP_1 and IP_2 disappear through the back ET and ionic dissociation (ID) to free anion and cation radicals, while no PT is observed. The efficiency of ID is greater in IP_2 (0.70) than in IP_1 (0.33). From temperature dependence on decay profiles, Arrhenius parameters are obtained for each decay process of the ion pairs. The PT process in BZ requires a considerably high activation energy (30 kJ mol^{-1}), while the ID process in DCE proceeds with practically no activation energy for both IP_1 and IP_2. The activation barrier for the back ET of IP_1 in BZ is obtained to be 13 kJ mol^{-1} which is significantly greater than that (~0 kJ Jmol^{-1}) in DCE. This solvent effect may be attributed to the difference in the ion pair states: i.e., a contact type in BZ and solvent-separated type in DCE.

Investigations concerning formation and decay dynamics of transient triplet ion pairs (^{3}IP) provide much information on many photochemical reactions associated with electron transfer (ET) in the triplet state.[1-9] In a previous work,[10] we have clarified decay characteristics of the triplet-state termolecular ion pairs (IP_2) between the chloranil anion radical ($CA^{\cdot-}$) and the dimer cation radical of naphthalene ($Np_2^{\cdot+}$) or monohalogenated naphthalenes ($NpX_2^{\cdot+}$) in DCE. It has been suggested that in the moderately polar DCE, IP_2 are in a loose, solvent-separated ion-pair (SSIP) state. If ^{3}IPs were produced in a nonpolar solvent such as BZ, they would be expected to be in a contact ion-pair (CIP) state and to exhibit a decay behavior notably different from that of SSIP, not only in a reaction mode but also in a rate of the back ET process. In BZ, however, the ion pair $^3(CA^{\cdot-}, Np_2^{\cdot+})$ is observed spectroscopically at only high [Np] (ca. 1 M),[6] which is in an equilibrium with $^3(CA^{\cdot-}, Np^{\cdot+})$ and also ^{3}CA over a wide concentration range of Np. As a result, the decay behavior of the each individual ion pair, $^3(CA^{\cdot-}, Np_2^{\cdot+})$ or $^3(CA^{\cdot-}, Np^{\cdot+})$, is rather complicated with respect to temperature dependence.[11] In addition, neither $^3(CA^{\cdot-}, NpX_2^{\cdot+})$ nor $^3(CA^{\cdot-}, NpX^{\cdot+})$ has been produced in BZ, whereas the locally excited (LE-type) triplet exciplexes, $^3(CA^*\cdots NpX)$, have been formed, because of relatively high ionization potentials of the halogenated naphthalenes. Then, we have tried to investigate various other systems yielding ^{3}IP. This report describes results of a detailed study on the decay dynamics of IP_1 for the CA-ACN system in both BZ and DCE together with decay characteristics of IP_2 observed in DCE. Difference in decay dynamics between CIP and SSIP is clarified

Experimental

An apparatus for measurements of transient absorption spectra and decay profiles was the same Nd:YAG laser system as used previously[10] operated in the third harmonic (355 nm) oscillation mode. The second harmonic at 532 nm was used for direct CT-band excitation. Some transient spectra were also observed by using a frequency doubled (347 nm) ruby laser system as described elsewhere.[3,12,13] The ground-state absorption spectra were recorded on a UV/VIS spectrophotometer (JASCO, Ubest-50) at room temperature. Acenaphthene (ACN; GR grade, Tokyo Kasei) was purified by recrystallization from a methanol-cyclohexane mixture and then from cyclohexane. Chloranil (CA: tetrachloro-*p*-benzoquinone) was the same material as purified previously.[10] Both spectrograde benzene (BZ, Dotite) and 1,2-dichloroethane (DCE, Dotite) were used as received. Sample solutions subject to the photolysis were deaerated carefully by Ar-bubbling for more than 15 min. Especially, for solutions of high [ACN] the Ar-bubbling was performed under the action of supersonic vibration in order to prevent the precipitation of ACN in a needle tube for the gas flow. Temperature control of a sample was performed by the same manner as described previously.[10]

Results and Discussion

The Ground-State Complex Formation and the Lowest CT-Band Excitation. A mixed solution of CA and ACN forms the electron donor-acceptor complex, CA···ACN, in the ground state. The complex exhibits the 1st charge-transfer (CT) absorption band with a maximum at 564 nm in DCE (Fig. 1) and at 558 nm in BZ (Fig. 2). The formation constant (K_c) and the molar extinction coefficient ($\varepsilon_c(\lambda)$) of the complex at the wavelength λ (nm) were estimated to be K_c= (0.63±0.01) M^{-1}; $\varepsilon_c(565)$=(1.59±0.03)×10^3 M^{-1} cm^{-1}

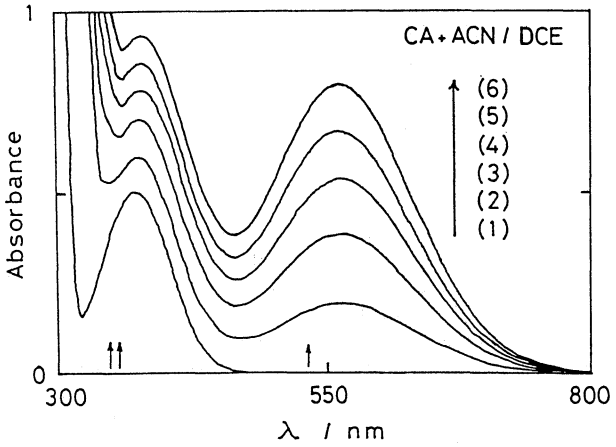

Fig. 1. The ground-state UV/VIS absorption spectra of the CA and ACN system in DCE: [CA]=2.09×10^{-3} M and [ACN]=(1) 0, (2) 0.100, (3) 0.200, (4) 0.300, (5) 0.400, and (6) 0.500 M. The short arrows indicate the wavelengths of the laser oscillation, 347, 355, and 532 nm.

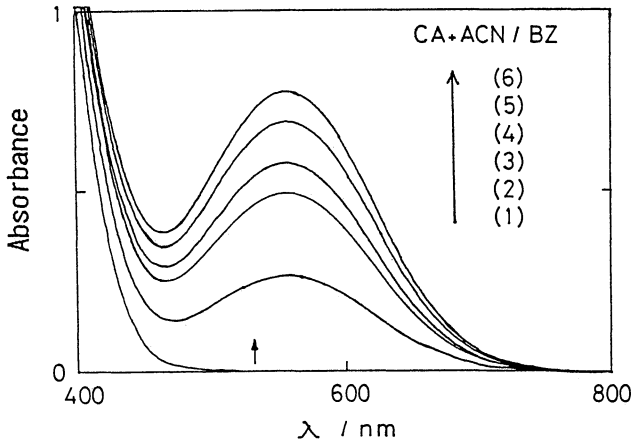

Fig. 2. The ground-state UV/VIS absorption spectra of the CA and ACN system in BZ: [CA]= 1.87×10^{-3} M and [ACN]=(1) 0, (2) 0.250, (3) 0.500, (4) 0.625, (5) 0.750, (6) 0.875 M.

in DCE at 25 °C and K_c=(0.31±0.01) M^{-1}; ε_c(560)= (1.95±0.07)×10^3 M^{-1}cm^{-1} in BZ at 25 °C. These values were obtained by the nonlinear least-square fitting using the following equation:[14]

$$D=(D_0+K_c[\mathrm{ACN}]D_c)/(1+K_c[\mathrm{ACN}]).$$

Here, D and D_0 are the absorbances in the presence and absence of ACN, respectively, under the conditions of [CA]≪[ACN]. D_c(=ε_c[CA], the light path l=1 cm) denotes the extrapolated absorbance of the complex in the infinite concentration of ACN; i.e., the absorbance of the complex when all CA is converted into the complex.

The laser pulse at 532 nm matches the 1st CT band of the complex in both solvents (indicated by short arrows in Figs. 1 and 2). However, the excitation at 532 nm led to no transient formation in both solvents

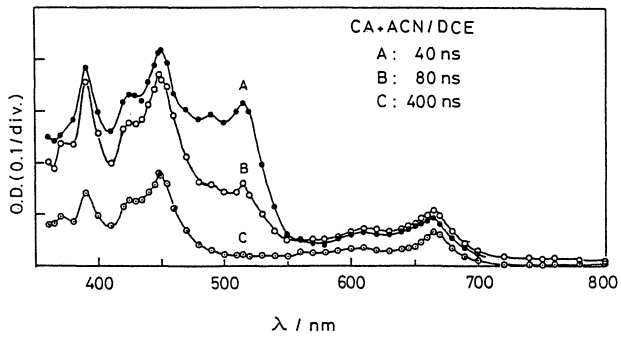

Fig. 3. Time-resolved transient absorption spectra of the CA (3.3×10^{-3} M) and ACN (3.2×10^{-3} M) system in DCE obtained by the ruby laser photolysis at 15 °C. Delay times after the start of laser oscillation are given in the figure.

even in the solutions containing the most concentrated ACN examined here (ca. 0.5 M in DCE and 1 M in BZ). This result indicates that the internal conversion in the S_1(CT) state of the complex is so rapid unable to be detected by nanosecond laser photolysis as reported previously for the CA-durene[1] and CA-diphenylamine[3] complexes.

Photolysis at 347 or 355 nm in DCE. As can be seen from Fig. 1, the second absorption band of the complex CA···ACN shorter than 450 nm overlaps with the band of CA having a maximum around 375 nm. The laser pulse at 347 or 355 nm can excite the band of free CA as well as the second band of the complex. Figure 3 shows time-resolved transient absorption spectra for the CA(3.3×10^{-3} M)-ACN(3.2×10^{-3} M) system in DCE obtained by the ruby laser photolysis. The band at 515 nm due to ^{3}CA[1,12] is quenched by ACN with a rate constant (k_q) expressed by the Arrhenius equation, k_q=5.1×10^{11}exp(−10.2 kJ mol^{-1}/RT) M^{-1}s^{-1}. This k_q value (e.g., 7.7×10^9 M^{-1}s^{-1} at 20 °C) is greater than that of 4.9×10^9 M^{-1}s^{-1} for the ET quenching by naphthalene (Np) at 20 °C.[10] This is due to low oxidation potential of ACN (1.25 eV)[15] than that of Np (1.65 eV).[15] The bands around 390, 450, and 665 nm appear remarkably associated with the ^{3}CA quenching. The 450-nm band is assigned as that of the chloranil radical anion (CA$^{\cdot-}$).[1] The bands around 390 and 665 nm are both characteristics of the acenaphthene radical cation (ACN$^{\cdot+}$).[16] Thus, the quenching reaction is surely ET from ACN to ^{3}CA occurring faster than that from Np in the CA-Np-DCE system.[10] These ion-radical bands decrease rapidly in an early stage (<200 ns after the excitation) and then decay with a relatively slow rate. Figure 4a gives a 1st-order decay profile of ^{3}CA monitored at 515 nm. Figure 4b shows 2nd-order decay plots corresponding to the bands of CA$^{\cdot-}$ at 448 nm and ACN$^{\cdot+}$ at 670 nm after the cessation of the initial rapid decay. The exactly 2nd-order kinetics of the ion-radical bands indicates clearly the formation of isolated CA$^{\cdot-}$ and ACN$^{\cdot+}$ decaying via recombination including

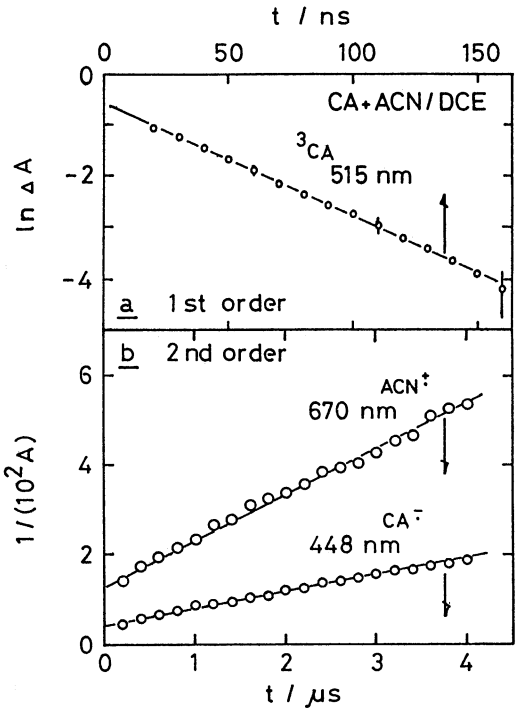

Fig. 4. Absorbance decay profile measured in the CA (3.3×10^{-3} M)-ACN (3.2×10^{-3} M)-DCE system at 15 °C: (a) ^{3}CA at 515 nm, (b) CA^- at 448 nm and ACN^+ at 670 nm.

back ET or disproportionation. The slope of the 2nd-order plots corresponds to $k_2/\varepsilon(\lambda)l$ where k_2 is the 2nd-order rate constant, $\varepsilon(\lambda)$ the extinction coefficient at λ, and l the optical path length. Therefore, the $\varepsilon(670)/\varepsilon(448)$ value can be evaluated to be 0.38. On the other hand, the value of $\varepsilon(670)/\varepsilon(448)$ is separately estimated to be 0.35 from the spectrum at 400 ns in Fig. 4. Both values are in good agreement with each other. On the assumption that the $\varepsilon(448)$ value mainly due to CA^- (the absorption of ACN^+ overlaps a little at 448 nm)[16] is approximated to 9.0×10^3 M^{-1} cm^{-1} of CA^-,[1] the $\varepsilon(670)$ value of ACN^+ is estimated as $(3.2—3.4)\times10^3$ $M^{-1}cm^{-1}$. This value is quite similar to $\varepsilon(685)$, $(3.0—3.2)\times10^3$ $M^{-1}cm^{-1}$, of Np^+.[17,18]

In order to observe clearly the rapid decay due to the ion pair, $^3(CA^-, ACN^+)$ or $^3(CA^-, ACN_2^+)$, as a precusor for the free ions, the photolysis was performed for the solutions containing more concentrated ACN. Figures 5, 6, and 7 present the transient spectra in the CA-ACN-DCE system at [ACN]=0.005, 0.1, and 0.3 M, respectively, measured at 8, 20, and 50 °C. At these concentrations, the ^{3}CA band around 515 nm is quenched almost completely immediately after the excitation. The spectra in Fig. 5 are mainly comprised of the characteristic bands of CA^- and the monomer ACN^+ in the present temperature range. Figure 6 shows the appearance of a new band around 580 nm instead of a relative decrease of the ACN^+ bands at 390 and 665 nm. The 580-nm band can be assinged as that of the acenaphthene dimer radical

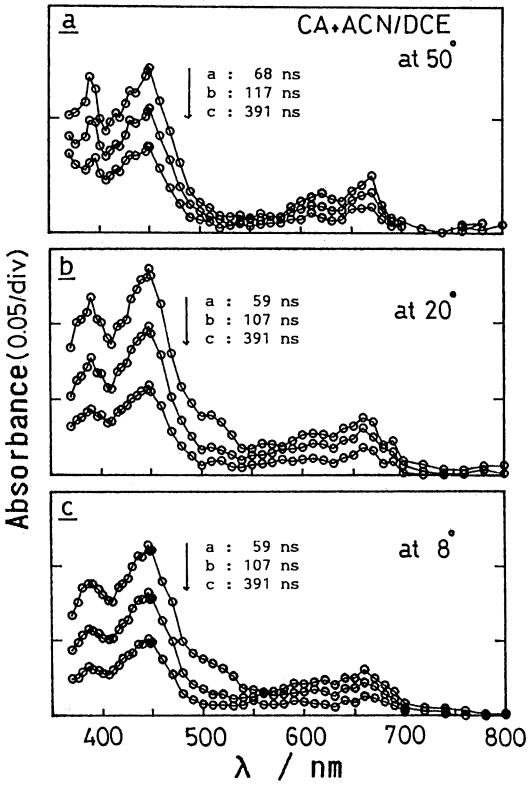

Fig. 5. Transient absorption spectra observed by the Nd : YAG laser system in the CA (2.0×10^{-3} M)-ACN (5.1×10^{-3} M)-DCE system at (a) 50, (b) 20, and (c) 8 °C. Delay times after the start of laser oscillation are given in the figures.

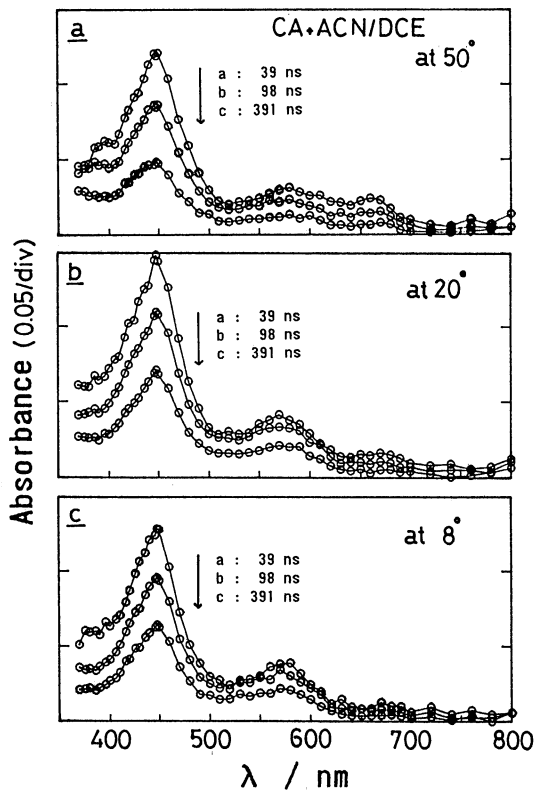

Fig. 6. Transient absorption spectra obseved in the CA (3.1×10^{-3} M)-ACN (0.10 M)-DCE system at (a) 50, (b) 20, and (c) 8 °C.

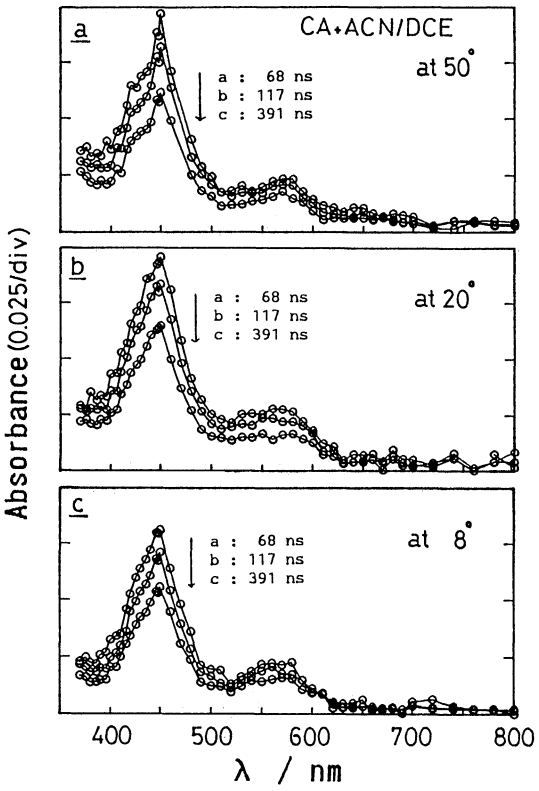

Fig. 7. Transient absorption spectra observed in the CA (2.0×10^{-3} M)-ACN (0.30 M)-DCE system at (a) 50, (b) 20, and (c) 8 °C.

cation, ACN_2^+, by comparison with a reported spectrum of ACN_2^+ in a freon matrix at 77 K[16] and that of Np_2^+ having a similar electronic structure.[10,17,18] These spectral features indicate that the dimer band relative to the monomer one increases in absorbance with an increase of [ACN] and with decreasing temperature. Similar spectral behavior was also observed in the solution containing 20 mM ACN. Such temperature dependence of the spectra implies that ACN_2^+ is energetically more stable than ACN^+ at least in the isolated state. The coexistence of ACN^+ and ACN_2^+ in the high concentration range suggests that the equilibrium constant between them is considerably small compared with that between Np^+ and Np_2^+.[10] In Fig. 7, the characteristic bands of CA^- and ACN_2^+ are observed remarkably even at the shortest delay time while no band due to ACN^+ is recognized almost completely. In addition, no CAH· formation is observed in DCE in the time range under the present concern (Figs. 3, 5—7). Therefore, no PT occurs competing with both ID and back ET in the ion pairs in DCE.

Figure 8 exemplifies decay profiles after one-shot excitation corresponding to the bands due to both CA^- at 448 nm (a) and ACN_2^+ at 580 nm (b) in the solution containing 0.1 M ACN. The smoose, dotted curves overlaid are calculated ones by the least-square method described later. These decay curves consist of two components. The initial, rapid decay is 1st order (the rate constant k_1) attributable to the decay of the ion pairs, $^3(CA^-, ACN^+)$ and/or $^3(CA^-, ACN_2^+)$. The slow component corresponds to the 2nd-order decay (the rate constant k_2) indicating the disappearance of the isolated ions, CA^-, ACN^+ and/or ACN_2^+. From Fig. 8, it is found that these two decay patterns resemble quite well and that the rate constant k_1 of the 448-nm band of CA^- is equal to that of the 580-nm band due to ACN_2^+ within experimental accuracy. This fact indicates that an equilibrium between $^3(CA^-,$

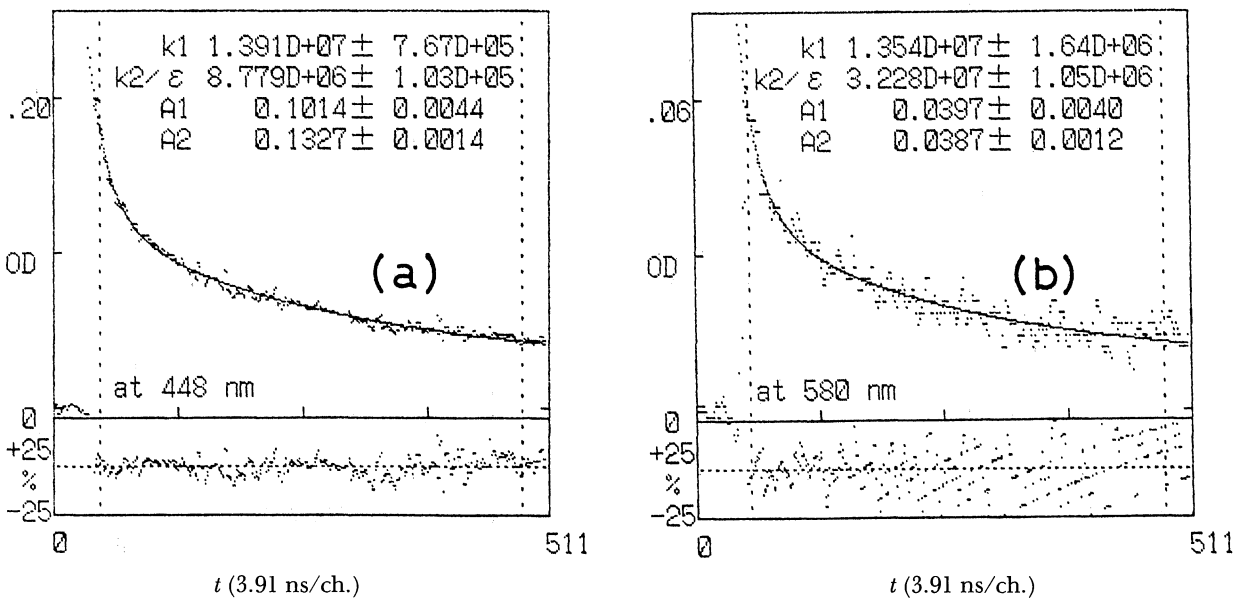

Fig. 8. Decay traces of absorbance due to CA^- at 448 nm (a) and ACN_2^+ at 580 nm (b) in the CA (3.0×10^{-3} M)-ACN (0.10 M)-DCE solution at 20 °C. The fitting was performed to the signal in the time range between two vertical, dotted lines. The residuals were plotted in the bottom. Owing to high [ACN], the fluorescence scattering could not be avoided in the present measurements immediately after the flash.

$ACN^{\ddagger}$) and $^3(CA^{\dot{-}}, ACN_2^{\ddagger})$ is established rapidly at such a high concentration of ACN (i.e., at least 0.1 M). Taking into consideration these temporal behaviors, most time-resolved spectra shown in Figs. 5—7 can be regarded as those of the ion pairs, although the spectra at the longest delay time correspond to those of the dissociated ions. Therefore, Fig. 5 shows the spectral change principally due to IP_1, $^3(CA^{\dot{-}}, ACN^{\ddagger})$, in the temperature range 8—50 °C. In contrast, Fig. 7 exhibits the spectral features dominantly due to IP_2, $^3(CA^{\dot{-}}, ACN_2^{\ddagger})$. Figure 6 shows spectra of an intermediate case involving both IP_1 and IP_2.

Estimation of Decay Parameters of the Ion Pairs in DCE. From the results mentioned above, ion-pair decay would be summarized as follows:

$$\begin{array}{ccccc} & & {}^3(CA^{\dot{-}}, ACN^{\ddagger}) + ACN & \longleftrightarrow & {}^3(CA^{\dot{-}}, ACN_2^{\ddagger}) \\ & kd^{(1)}\downarrow & \downarrow ki^{(1)} & ki^{(2)}\downarrow & \downarrow kd^{(2)} \\ (CA, ACN) & & CA^{\dot{-}}+ACN^{\ddagger}+ACN & \longleftrightarrow & CA^{\dot{-}}+ACN_2^{\ddagger} \quad (CA, ACN_2) \\ & \downarrow & k_2^{(1)}\downarrow & \downarrow k_2^{(2)} & \downarrow \\ CA+ACN & & CA+2ACN & & CA+2ACN \\ & & \text{or other products} & & \end{array}$$

Scheme 1.

where $kd^{(n)}$ and $ki^{(n)}$ are the rate constants for the back ET to the ground state and the ionic dissociation to the corresponding free ions, respectively. The superscript n (1 or 2) indicates each quantity belonging to IP_1 or IP_2, respectively. If the equilibrium between IP_1 and IP_2 is established dynamically or inclines to the one side of the equilibrium as mentioned previously at 5×10^{-3} or 0.3 M of ACN, then the kinetic analysis for such cases would be sufficient to take into account only decay processes for apparently one triplet ion pair (^3IP). Therefore, rate equations for ^3IP and the free ions (FI) can be expressed as follows:

$$d[^3IP]/dt = -(ki+kd)[^3IP] \quad (1)$$

$$d[^3FI]/dt = ki[^3IP] - k_2[FI]^2 \quad (2)$$

The observed absorbance D, which is the sum of absorbances of ^3IP and FI, is given by Eq. 3:

$$dD/dt = -[1-(\varepsilon_2/\varepsilon_1)\phi i]\, k_1 D_0 \exp(-k_1 t) - (k_2/\varepsilon_2)[D - D_0\exp(-k_1 t)]^2 \quad (3)$$

where $k_1=ki+kd$, $\phi i=ki/(ki+kd)$, ε_1 and ε_2 refer to the extinction coeficients of ^3IP and FI respectively at the observed wavelength λ, and D_0 denotes the initial value of D at $t=0$. Here, the optical path length l is settled to be unity for simplicity. This situation is just the same as that for $^3(CA^{\dot{-}}, Np_2^{\ddagger})$ in the CA-Np-DCE system reported previously.[10] Therefore, we can analyze decay curves by the same approximation method as utilized for $^3(CA^{\dot{-}}, Np_2^{\ddagger})$,[10] instead of using the complicated solution of Eq. 3.[20] The approximate solution of Eq. 3 is given by the follwing equation:

$$D = A_1\exp(-k_1 t) + 1/[(1/A_2)+(k_2/\varepsilon_2)t] \quad (4)$$

where A_1 and A_2 are the initial absorbances of the independently decaying two components, M_1 with the 1st-order rate constant k_1 and the extinction coefficient ε_1 and M_2 with the 2nd-order rate constant k_2 and ε_2, respectively. In this model, the value $(\varepsilon_1/\varepsilon_2)A_2/(A_1+A_2)$ is assumed to correspond to ϕi. The differential of Eq. 4 has the following form (Eq. 5), which is rather similar to Eq. 3:

$$dD/dt = -[1-(\varepsilon_2/\varepsilon_1)\phi i]\, k_1 D_0\exp(-k_1 t) - (k_2/\varepsilon_2)\{D - [1-(\varepsilon_2/\varepsilon_1)\phi i]\, D_0\exp(-k_1 t)\}^2 \quad (5)$$

In the present case, ε_1 may be nearly equal to ε_2 because of spectral similarity between ^3IP and FI.

The dotted curves in Fig. 8 are fitting ones obtained by the nonlinear least-square regression analysis (Marquardt method) using Eq. 4. The agreement between the observed and calculated curves is excellent. It has been found previously that the parameters, k_1, k_2/ε_2, and ϕi, estimated by this approximation can be utilized as reliable parameters for the real kinetics (Eq. 3)[10] Accordingly, we can obtain the decay rate constants, ki and kd, from the relations, $ki=k_1\phi i$ and $kd=k_1(1-\phi i)$, for individual ion pairs. This approximation method was also applicable to the decay curves at various [ACN].

Figure 9 shows k_1 values as a function of [ACN] obtained by this method applied to the decay curves at 448 nm. The k_1 value is nearly constant in the range $[ACN]=(0.5-2)\times10^{-2}$ M and tends to decrease slightly with an increase of [ACN] up to 0.3 M. Unfortunately, it was impossible to measure accurately the k_1 values at [ACN] > 0.3 M, because the intensity of transient absorption became extremely weak owing to strong overlap of the CT band of CA···ACN with the band of free CA at 355 nm for excitation. It was additionally found that, simultaneously with the change of k_1, the ϕi value tends to increase with an increase of [ACN] in the $(2-10)\times10^{-2}$ M range. The plateau region of k_1 in the low [ACN] corresponds to the IP_1 region. From this result together with the result of temperature independence of the IP_1 spectrum (Fig. 5), the 1st-order decay rate constants k_1 obtained in the solution containing 5×10^{-3} M ACN can be regarded as intrinsic ones of IP_1 independent on the equilibrium between IP_1 and IP_2 at the temper-

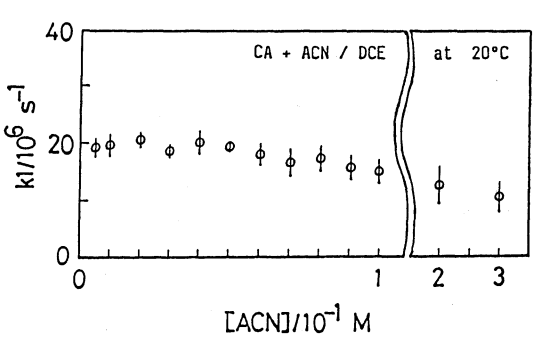

Fig. 9. Plots of the k_1 values as a function of [ACN].

Table 1. Decay Kinetic Prameters (at 20 °C) of (1 : 1) and (1 : 2) Ion Pairs Obtained in the CA-ACN-DCE System

(Ion pair)	ϕi	k_1	ki	kd
			$10^6\ s^{-1}$	
(1 : 1)[a]	0.33±0.04	19±2	6±1	13±2
E_a/kJ mol^{-1}			2.3±0.6	0.3±1.2
log(A/s^{-1})			7.2±0.1	7.1±0.2
(1 : 2)[b]	0.70±0.03	13±3	9±3	4±1
E_a/kJ mol^{-1}			−0.3±2.3	5.4±2.8
log(A/s^{-1})			6.9±0.4	7.5±0.5

a) $^3(CA^{\cdot-}, ACN^{\dagger})$; [ACN]=5.1×10^{-3} M. b) $^3(CA^{\cdot-}, ACN_2^{\dagger})$; [ACN]=0.30 M.

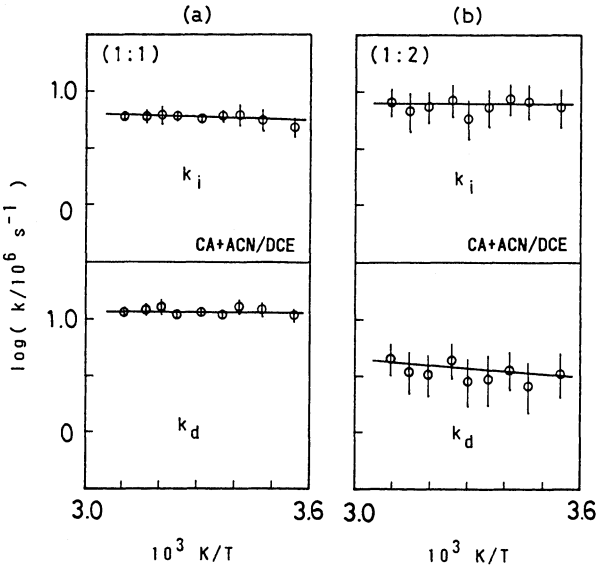

Fig. 10. Arrhenius plots for the ki and kd values of the ion pairs: (a) $^3(CA^{\cdot-}, ACN^{\dagger})$ in the solution containing [CA]=2.0×10^{-3} and [ACN]=5.1×10^{-3} M; (b) $^3(CA^{\cdot-}, ACN_2^{\dagger})$ in the solution of [CA]=2.0×10^{-3} and [ACN]=0.30 M in DCE.

atures 8—50 °C. At first glance, on the other hand, the k_1 value at [ACN]=0.3 M does not appear to reach a limiting value of IP_2 in Fig. 9. However, it would be reasonable that the k_1 value at 0.3 M is nearly equal to that of IP_2 itself, since IP_2 exists dominantly in the solution of 0.3 M ACN (Fig. 7) and the k_1 value of IP_1 is not so great as to affect largely the decay rate of IP_2 at such a negligibly small fraction of IP_1 in the equilibrium, if any. Hence, the decay rate parameters of IP_1 and IP_2 can be estimated from the analysis for the solutions containing 5.1×10^{-3} and 0.30 M ACN, respectively.

Temperature effects on ki and kd for each ion pair are plotted in Fig. 10. Table 1 presents the kinetic parameters for the ion pairs at 20 °C together with the Arrhenius parameters. In Table 1, on going from IP_1 to IP_2, the ki value becomes somewhat large but the kd value decreases into about one third at 20 °C. This result explains the tendency that with increasing [ACN], k_1 becomes small and inversely ϕi becomes large. The activation energies (E_a) are very small for both ID and back ET in each ion pair. The fact that virtually no activation energy is required for ki indicates that the geminate ion radicals are bound very weakly. Hence, they are considered to be spatially separated from each other in a solvent cage by a solvation weakening the Coulomb attraction between them. These properties of the ion pairs are quite similar to those of the (1 : 2) ion pair, $^3(CA^{\cdot-}, Np_2^{\dagger})$ in DCE, which has been suggested to be a loose SSIP.[10] Therefore, it is also suggested that the ion pairs observed here in DCE exist dominantly as SSIP. Then, it is additionally understood that the spectra of the ion pairs are very similar to those of the free ions. Other properties of the ion pairs will be compared later with those of an ion pair in BZ.

Photolysis in Bz. This solvent system has been studied by Jones et al.[9] concerning mainly intra-ion-pair proton transfer (PT) in a limited concentration (≦20 mM) of ACN at 25 °C. We have investigated here the same system in a more wide [ACN] range (≦1.0 M) and temperature effect has been examined with special attention to the back ET process rather than the PT reaction. The triplet chloranil ^3CA in BZ which exists in the complexed state, $^3CA\cdots BZ$,[21,22] is quenched by ACN with a rate constant expressed by $k_q=(5.6\pm1.2)\times10^8\exp[-(11.0\pm0.4)\ \text{kJ mol}^{-1}/RT]\ M^{-1}s^{-1}$ in the range 8—50 °C. the k_q value of 6.0×10^9 M^{-1}s^{-1} in BZ at 20 °C is smaller than that of 7.7×10^9 M^{-1}s^{-1} in DCE in harmony with the effect of solvent polarity on ET quenching. Figure 11 shows time-resolved transient absorption spectra for the CA-ACN system in BZ involving various concentrations of ACN. A strong band around 450 nm and a relatively weak, broad band around 650 nm are observed immediately after the ^3CA quenching. With increasing delay time, the strong band decays rapidly causing a peak shift from 450 to 435 nm. The 435 nm band disappears gradually with a long life. On the other hand, the band around 650 nm decays rapidly in a monotonous fashion.[23] The initial band around 450 nm is identified as that of $CA^{\cdot-}$ in BZ from comparison with the reported spectra[22] and that in various solvents.[1,2,12,13] Hence, the band around 650 nm is assignable to that of the counter cation radical, $ACN^{\dagger}$, taking additionally acount of the spectral similarity with that in DCE. However, the spectrum of $ACN^{\dagger}$ in BZ is significantly broad and shifts to blue by ca. 20—30 nm in comparison with that in DCE. These spectral features (shift and broadening) seem to result from the electrostatic and/or exchange interaction between $CA^{\cdot-}$ and $ACN^{\dagger}$ in a close contact state, although solvation effect by BZ with π electrons would also contribute to the broadening in some degree. Similar solvent effect on transient spectra has been known for a typical singlet exciplex between pyrene and diethylaniline[24] and the pyrene-dimethylaniline

intramolecular exciplex.[25] Then, it is considered that both ions, $CA^{\cdot-}$ and $ACN^{\cdot+}$, exist as a contact ion pair as expected. In fact, their decay profiles obey exactly the 1st-order kinetics as shown later. The band at 435 nm is assigned as that of CAH·, because its spectrum is similar to that of CAH· in BZ produced via hydrogen transfer reaction between ^{3}CA and tetrachlorohydroquinone.[13,26] No long-lived free ions, $CA^{\cdot-}$ and $ACN^{\cdot+}$, were recognized in the spectra in BZ (Fig. 11) unlike those in DCE (Figs. 5—7). This result indicates that no ID occurs in BZ. These spectral features in Fig. 11 are well similar to one another and essentially independent on temperature variation as examined in the solution of 4×10^{-2} M ACN as an example. No absorption band due to the dimer cation radical $ACN_2^{\cdot+}$ can be observed even at 1 M ACN (Fig. 11d). Since the spectrum of $Np_2^{\cdot+}$ is observed in BZ at 1.0 M Np,[6,11] the present result indicates that due to the steric hindrance the formation of $ACN_2^{\cdot+}$ from the corresponding monomer cation radical is less efficient than that of $Np_2^{\cdot+}$ in BZ as well as in DCE.

It should be noted here that the formation process of CAH· would not be an ultrafast hydrogen-transfer (HT) reaction from an encounter complex between ^{3}CA and ACN competing with ^{3}IP formation, although such a mechanism has been reported for a few similar systems.[1,5,27] Reasons for this neglect are the followings. (1) In the mechanism of such a rapid HT,[1] it is presumed naturally that yields of neutral radicals are insensitive to solvent polarity. In fact, it has been confirmed in the benzophenone-diphenylamine system.[27] In the present case, however, the CAH· formation is remarkably dependent on the solvent, BZ or DCE. (2) In the rapid HT, the relative yields of neutral radicals and ^{3}IP would be expected also to be less dependent on temprature. However, it was found that the yield of CAH· estimated by the comparison with a reference absorbance of ^{3}CA was significantly dependent on temperature as well as the yield ϕr defined below. Therefore, it is considered that CAH· is originated successively from ^{3}IP.

Reaction pathways of the ion pair, $^3(CA^{\cdot-}, ACN^{\cdot+})$, can be written by the following scheme:

$$\begin{array}{ccc} & {}^3(CA^{\cdot-}, ACN^{\cdot+}) & \\ & k\mathrm{d}\downarrow \qquad \downarrow k\mathrm{r} & \\ CA + ACN \leftarrow (CA, ACN) & & CAH\cdot + ACN'\cdot \xrightarrow{k_2} \text{products} \end{array}$$

Scheme 2.

where kd is the rate constant of back ET accompanying spin inversion, kr the rate constant of proton transfer leading to the production of neutral free radicals, and k_2 the 2nd-order rate constant of the radicals via recombination or disproportionation. ACN'· represents acenaphthenyl radical. Although ACN'· has a strong characteristic absorption band at 380 nm,[28] no band could be observed owing to the internal filter effect by the intense absorption of the CA···BZ complex (Fig. 2). This scheme is essentially the same as that presented by Jones et al.[8] and similar

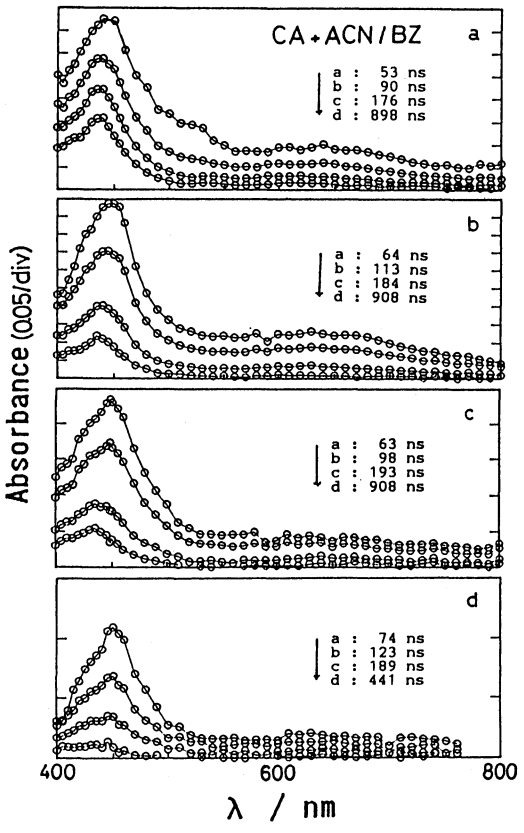

Fig. 11. Time-resolved transient absorption spectra for the CA and ACN systems in BZ at 20 °C: [CA]=1.93×10^{-3} M and [ACN]=(a) 4.99×10^{-3}, (b) 4.08×10^{-2}, (c) 0.50, (d) 1.00 M.

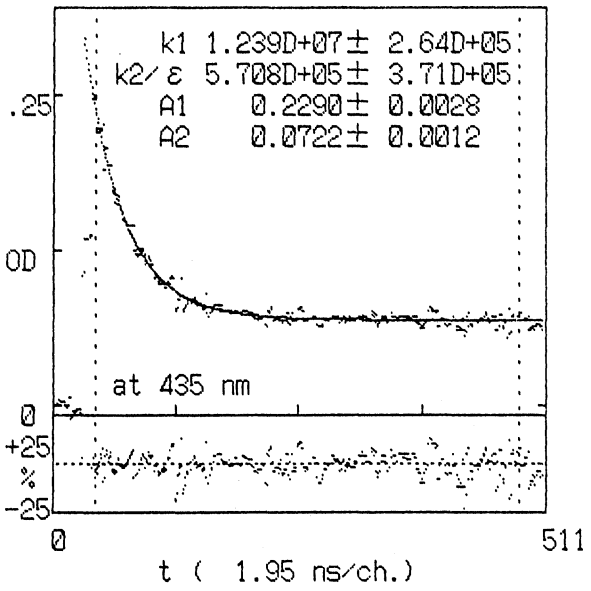

Fig. 12. Decay profile of transient absorbance at 435 nm measured in the CA (1.95×10^{-3} M)-ACN (2.00×10^{-2} M)-BZ solution at 20 °C.

in form to the decay pathways of the individual ion pairs in Scheme 1. Different points of Scheme 2 from Scheme 1 are the reactions producing the neutral radicals and successive product formation.[8] Therefore, the same kinetic analysis as mentioned above is applicable. Transient decay monitored at 435 nm is exemplified in Fig. 12, where the dotted curve is also a fitting one according to Eq. 4. Here, $k_1=kd+kr$ and $\phi r=kr/(kd+kr)=(\varepsilon_1/\varepsilon_2)A_2/(A_1+A_2)$. Namely, the first, rapid decay component is due to the ion pair obeying the 1st-order kinetics (k_1) and the second, slow component is attributed to the 2nd-order decay (k_2) of the free radicals, mainly CAH·. In this case, the value of ε_1 is not equal to that of ε_2. For estimation of ϕr, we use here $\varepsilon_1(435)=6.2\times10^3$ $M^{-1}cm^{-1}$ of $CA^{\cdot-}$ in acetone[29] and $\varepsilon_2(435)=5.7\times10^3$ $M^{-1}cm^{-1}$ of CAH· in BZ estimated by spectral comparison with that in dioxane.[13,26,30] The decay rate constant k_1 was independent on [ACN] in the range 5×10^{-3}—0.25 M. Judging from the above-mentioned spectral and kinetic features, it seems that the ion pair exists in the (1 : 1) type, $^3(CA^{\cdot-}, ACN^{\ddagger})$, at least in this [ACN] region. Then, we examined temperature effect upon the ion-pair decay using the solutions of $(1—4)\times10^{-2}$ M ACN. Arrhenius plots for kd and kr are illustrated in Fig. 13. Averaged results are listed in Table 2, where the result for the system containing 1.0 M ACN at 20 °C is additionally given.

Table 2. Decay Kinetic Prameters (at 20 °C) of (1 : 1) and (1 : 2) Ion Pairs Obtained in the CA-ACN-BZ System

(Ion pair)	ϕr	k_1	kr	kd
			10^6 s^{-1}	
(1 : 1)[a]	0.25±0.05	12.5±1.4	3.2±1.1	9.3±1.8
E_a/kJ mol^{-1}			29.8±0.8	13.2±0.6
log (A/s^{-1})			11.8±0.1	9.3±0.1
(1 : 1)+(1 : 2)[b]	0.06±0.01	11.4 ±0.7	0.7±0.2	10.7±0.8

a) $^3(CA^{\cdot-}, ACN^{\ddagger})$; [ACN]=(1—4)×10^{-2} M. b) $^3(CA^{\cdot-}, ACN^{\ddagger})$+$^3(CA^{\cdot-}, ACN_2^{\ddagger})$; [ACN]=1.0 M.

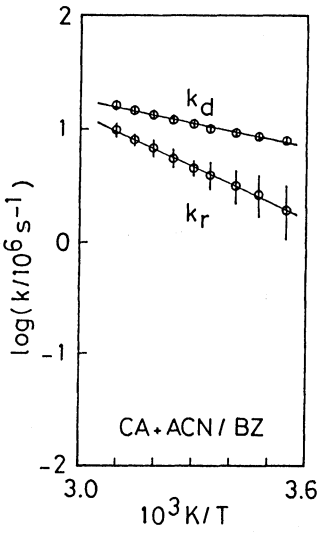

Fig. 13. Arrhenius plots for kr and kd values of the (1 : 1) ion pair, $^3(CA^{\cdot-}, ACN^{\ddagger})$ in BZ.

Comparison of Decay Characteristics between the Ion Pairs in BZ and DCE. As mentioned above, the observed triplet ion pairs (^{3}IP) may exist principally as the contact ion pair (CIP) in BZ and the solvent-separated ion pair (SSIP) in DCE. From the viewpoint of the ion-pair states, the decay properties in Tables 1 and 2 can be understood. The ionic dissociation of ^{3}IP occurs in DCE with a rate constant of several 10^6 s^{-1} but does not occur in nonpolar BZ, since the contact ^{3}IP in BZ is strongly bound by Coulomb force. Some ki values in DCE are known to be (12, 9, 7, 6, and 7)×10^6 s^{-1} for the (1 : 2) ion pairs, $^3(CA^{\cdot-}, Np_2^{\ddagger})$, $^3(CA^{\cdot-}$, (1-chloronaphthalene)$_2^{\ddagger})$, $^3(CA^{\cdot-}$, (2-chloronaphthalene)$_2^{\ddagger})$, $^3(CA^{\cdot-}$, (1-bromonaphthalene)$_2^{\ddagger})$, and $^3(CA^{\cdot-}$, (2-bromonaphthalene)$_2^{\ddagger})$, respectively,[10] and (5 and ca. 10)×10^6 s^{-1} for the (1 : 1) ion pairs, $^3(CA^{\cdot-}$, durene$^{\ddagger})$ and $^3(CA^{\cdot-}$, diphenylamine$^{\ddagger})$, respectively.[1,3] Thus, the ki value of SSIP is not so dependent on the difference of the cation radical species, although it may be affected slightly by the ion size or molecular weight.

In contrast, the proton transfer (PT) takes place in BZ but does not in DCE. The activation energy in PT is distinctly large and common for such kinds of PT[5]. This marked contrast in reactivity between CIP and SSIP may result from the essential difference in a separation distance between geminate anion and cation radicals. Namely, in CIP a special conformation required for PT would be established easily by the mutual orientation but in SSIP such a conformation may be restricted, because the geminate ions in SSIP are separated by solvent molecules from each other with a relatively long distance. Therefore, even if PT occurred in DCE, it would proceed with a very low frequency factor. Although it is known that a similar type of PT occurs competing with ID in $^3(CA^{\cdot-}$, durene$^{\ddagger})$ with a rate constant of 2×10^6 s^{-1} in DCE at 20 °C,[1] this discripancy between $^3(CA^{\cdot-}, ACN^{\ddagger})$ and $^3(CA^{\cdot-}$, durene$^{\ddagger})$ would be resolved by taking into account the differences in the number of active hydrogens and in properties of the proton donors; i.e., $ACN^{\ddagger}$ is a relatively weak proton donor judging from both acidity of the cation radicals and stabilization energy of the resultant neutral radicals. The high frequency factor (ca. 10^{12} s^{-1}) for kr in BZ seems appropriate to the intra-ion-pair PT without spin inversion.

As can be seen from Fig. 11d and Table 2, the yield of CAH· decreases remarkably in the solution containing 1.0 M ACN in BZ. This behavior is found to be attributed mainly to decrease in kr but not to increase in kd. At such a high [ACN], some interaction of the (1 : 1) ^{3}IP with the excess ACN could not be neglected. The interaction is assumed to be a weak (1 : 2) ^{3}IP formation although it is unclear from the spectra. In

this respect, similar low yields of CAH· and k_r values were found in experiments using cis and trans dimers of acenaphthylene with a weak electronic interaction between two acenaphthene rings as donors.[11] Therefore, it is considered that the decrease in the PT rate is caused from a reduction in acidity of a hydrogen at 9- or 10-position of ACN^{+} induced by a weak resonance interaction between the acenaphthene rings.

In Table 1 for SSIP, the k_d value (13×10^6 s^{-1}) of the (1:1) $^3(CA^{-}, ACN^{+})$ is greater than that (4×10^6 s^{-1}) of the (1:2) $^3(CA^{-}, ACN_2^{+})$. The latter value is also smaller than the k_d value (10×10^6 s^{-1}) of the (1:2) $^3(CA^{-}, Np_2^{+})$[10] which is rather close to the former. Furthermore, the k_d value of $^3(CA^{-}, ACN^{+})$ is nearly equal to that (13×10^6 s^{-1}) of $^3(CA^{-}, durene^{+})$ in DCE.[1] The oxidation potentials of a donor (D), $E(D/D^{+})$, are known to be 1.25 V for ACN, 1.65 V for Np, and 1.59 V for durene,[15] and estimated to be 1.1 V for the dimer Np_2 in the ground state.[31] From the fact that $(ACN)_2^{+}$ shows the absorption band very similar to that of Np_2^{+}, it might be estimated that $(ACN)_2$ in the ground state also has the oxidation potential approximately close to that (1.1 V) of Np_2. It has been reported that the back ET processes in some EDA systems with energetics similar to those in the present case belong to the Marcus "inverted region" in the nonpolar BZ (dielectric constant ε=2.28) and less polar 1,1,2,2-tetrachloroethane (ε=8.2).[4] However, taking the $E(D/D^{+})$ values into consideration in the present work, the above-noted results in DCE (ε=10.66) can not be interpreted by the energy gap law in the "inverted region". Therefore, the back ET of the present SSIP in DCE may be considered to proceed through singlet-triplet transition enhancement in the ion radical pair by the hyperfine coupling mechanism or others as known in the magnetic field effect on various radical and ion pairs in polar solvents;[32-34] that is, the indirect back ET via the singlet ion-pair state. This consideration does not contradict the fact that the activation energies (E_a) are practically zero for k_d as well as k_i, since in such a case the rate-determining spin-inversion process, $^3IP \rightarrow {}^1IP$, requires practically no activation energy.

On the other hand, the back ET process of $^3(CA^{-}, ACN^{+})$ in BZ requires a distinct activation energy (13 kJ mol^{-1}). This E_a value is reasonable as the activation energy for the intra-ion-pair transition, since similar activation energies have been reported for the intersystem crossing or internal conversion in some aromatic hydrocarbons with a naphthalene ring.[28,35-38] For the contact $^3(CA^{-}, ACN^{+})$ in BZ its energy level can be estimated to be 1.40 eV above the ground state by the following equation:[1,22]

$$E(CT) = E(ACN/ACN^{+}) - E(CA^{-}/CA) + 0.16 \quad (6)$$

Then, the k_d value of 9×10^6 s^{-1} in this system lies well on the line in the "inverted region" of the k_d vs. ΔG (free energy change) relationship in BZ.[4] Therefore, if the energy splitting between the singlet and triplet states is fairly large in this CIP[39] as noted previously by Levin et al. for the CA-durene or -hexamethylbenzene system,[22] then the back ET of $^3(CA^{-}, ACN^{+})$ in BZ can be regarded as the direct transition to the ground state.

Summary

1) Both (1:1) and (1:2) triplet ion pairs, $^3(CA^{-}, ACN^{+})$ and $^3(CA^{-}, ACN_2^{+})$, were found to behave as solvent-separated ion pairs in moderately polar DCE. The ion pairs decay through ionic dissociation (ID) and back electron transfer (ET). The activation energies of ID and back ET processes are virtually zero for both ion pairs.

2) The (1:1) ion pair in BZ behaves as a contact ion pair, which decays via back ET and proton transfer (PT). The back ET requires a small but definite activation energy (13 kJ mol^{-1}). The PT process in the contact ion pair takes place with a considerable activation barrier of 30 kJ mol^{-1}.

3) Such discrimination of the ion-pair types was established by examining spectral features and temperature dependence of decay channels (ID,PT, and back ET) as probes.

4) Mechanism of the back ET in the triplet ion pairs (direct or indirect pathway connecting with more detailed mechanisms such as spin-orbit coupling, hyperfine coupling, and others) seems to be swayed by a delicate balance of distribution between contact and solvent-separated ion pairs in an equilibrium state.

References

1) H. Kobashi, M. Funabashi, T. Kondo, T. Morita, T. Okada, and N. Mataga, *Bull. Chem. Soc. Jpn.*, **57**, 3557 (1984).

2) H. Kobashi, T. Kondo, and M. Funabashi, *Bull. Chem. Soc. Jpn.*, **59**, 2347 (1986).

3) H. Kobashi, M. Funabashi, H. Shizuka, T. Okada, and N. Mataga, *Chem. Phys. Lett.*, **160**, 261 (1989).

4) P. P. Levin, P. F. Pluzhnikov, and V. A. Kuzmin, *Chem. Phys. Lett.*, **147**, 283 (1988).

5) P. P. Levin, T. A. Kokrashvili, and V. A. Kuzmin, *Bull. Acad. Sci. USSR, Div. Chem. Sci.*, **32**, 251 (1983).

6) V. A. Kuzmin and P. P. Levin, *Bull. Acad. Sci. USSR, Div. Chem. Sci.*, **37**, 429 (1988).

7) G. Jones, II and W. A. Haney, *J. Phys. Chem.*, **90**, 5410 (1986).

8) G. Jones, II, W. A. Haney, and X. T. Phan, *J. Am. Chem. Soc.*, **110**, 1922 (1988).

9) G. Jones, II and K. Mouli, *J. Phys. Chem.*, **92**, 7174 (1988).

10) H. Kobashi, H. Suto, and H. Shizuka, *Bull. Chem. Soc. Jpn.*, **63**, 1441 (1990).

11) H. Kobashi, Y. Ohsugi, S. Okabe, and H. Shizuka, to be published.

12) H. Kobashi, H. Gyoda, and T. Morita, *Bull. Chem. Soc. Jpn.*, **50**, 1731 (1977).

13) H. Kobashi, Y. Tomioka, and T. Morita, *Bull. Chem. Soc. Jpn.*, **52**, 1568 (1979).
14) Equation 1 is equivalent to the Benesi-Hildebrand-Ketelaal equation.
15) K. L. Weinberg and H. R. Weinberg, *Chem. Rev.*, **68**, 449 (1968); T. A. Gough and M. E. Peover, "Polarography," Macmillan, London (I967), Vol. 2, p. 1017.
16) T. Shida and S. Iwata, *J. Am. Chem. Soc.*, **95**, 3473 (1973).
17) A. Kira, T. Nakamura, and M. Imamura, *J. Phys. Chem.*, **81**, 511 (1977).
18) R. Gschwind and E. Haselbach, *Helv. Chim. Acta*, **62**, 941 (1979).
19) E. F. Hillinsky, S. V. Milton, and P. M. Rentzepis, *J. Am. Chem. Soc.*, **105**, 5193 (1983).
20) J. -Y. Chien, *J. Am. Chem. Soc.*, **70**, 2256 (1948).
21) K, Kawai, Y. Shirota, H. Tsubomura, and H. Mikawa, *Bull. Chem. Soc. Jpn.*, **45**, 77 (1972).
22) P. P. Levin, P. F. Pluzhnikov, and V. A. Kuzmin, *Bull. Acad. Sci. USSR, Div. Chem. Sci.*, **38**, 167 (1989); *Chem. Phys. Lett.*, **152**, 409 (1988).
23) A very weak residual absorption remains with a long life around 650 nm but we can not assign it at the present stage of the investigation.
24) H. Fujiwara, N. Nakashima, and N. Mataga, *Chem. Phys. Lett.*, **47**, 185 (1977).
25) J. Hinatu, H. Masuhara, N. Mataga, Y. Sakata, and S. Misumi, *Bull. Chem. Soc. Jpn.*, **51**, 1032 (1978).
26) H. Kobashi, T. Nagumo, and T. Morita, *Chem. Phys. Lett.*, **57**, 369 (1978) and unpublished results.
27) H. Miyasaka and N. Mataga, *Bull. Chem. Soc. Jpn.*, **63**, 131 (1990).
28) H. Kobashi, H. Ikawa, R. Kondo, and T. Morita, *Bull. Chem. Soc. Jpn.*, **55**, 3013 (1982).
29) Y. Iida, *Bull. Chem. Soc. Jpn.*, **43**, 2772 (1970).
30) S. K. Wong, L. Fabes, W. J. Green, and J. K. S. Wan, *J. Chem. Soc., Faraday Trans. 1*, **68**, 2211 (1972).
31) H. Beens and A. Weller, *Chem. Phys. Lett.*, **2**, 140 (1968).
32) K. Shulten, H. Staerck, A. Weller, H. J. Werner, and B. Nickel, *Z. Phys. Chem. (Frankfurt am Main)*, **101**, 371 (1976).
33) H. Hayashi and S. Kagakura, *Bull. Chem. Soc. Jpn.*, **57**, 322 (1984).
34) P. P. Levin, I. V. Khudyakov, and V. A. Kuzmin, *J. Phys. Chem.*, **93**, 208 (1989).
35) J. B. Birks, "Photophysics of Aromatic Molecules," Wiley-Interscience, London (1970).
36) S. G. Hadley, H. E. Rast, Jr., and R. A. Keller, *J. Chem. Phys.*, **39**, 705 (1963).
37) R. E. Kellogg and R. P. Schwenker, *J. Chem. Phys.*, **41**, 2860 (1964).
38) R. B. Cundall and L. C. Pereira, *Chem. Phys. Lett.*, **15**, 383 (1972).
39) The energy level of $^1(CA^{\overline{\cdot}}, ACN^{\dagger})$ may be estimated to be ca. 1.65 eV from the long wavelength edge of the CT band. Then, the S-T splitting is calculated as ca. 24 kJ mol^{-1} which is larger than the E_a value (13 kJ mol^{-1}).